An application of fuzzy-evolutive integral to improve the performances of multispectral ATR systems

Constantin-Iulian VIZITIU, Florin ŞERBAN, Teofil OROIAN, Cristian MOLDER, Mihai STANCIU
Communications and Electronic Systems Department
Military Technical Academy
George Cosbuc Avenue 81-83, 5th District, Bucharest
ROMANIA
vic@mta.ro florin.serban@ascr.ro oroiant@mta.ro mcc@mta.ro mst@mta.ro http://www.mta.ro

Abstract: - According to the literature assigned to automatic target recognition (ATR) system theory, one of the most important methods to improve the performances of these is to use multispectral information provided by a suitable set of sensors, and certainly, proper information fusion techniques. In this paper authors propose an application using an improved evolutive version of Sugeno's fuzzy integral to increase the target recognition performances based on high-resolution radar (HRR) and video imaginary. In order to confirm the broached theoretical aspects, a real input database was used.

Key-Words: - ATR systems, HRR/video imaginary, decision fusion, neural networks

1 Introduction

The *high-resolution radar range profiles* (HRRP) are often used inside of multispectral ATR systems. Generally speaking, a range profile of a target can be regarded as its 1D signature, generated by the electromagnetic reflection of a high-frequency broadband signal. It is obtained as the projection of the target scattering points, defining the *high-resolution chart* of target, on the radar line of sight [1], [2]. An example how can obtain the radar target profile is presented in Fig.1.

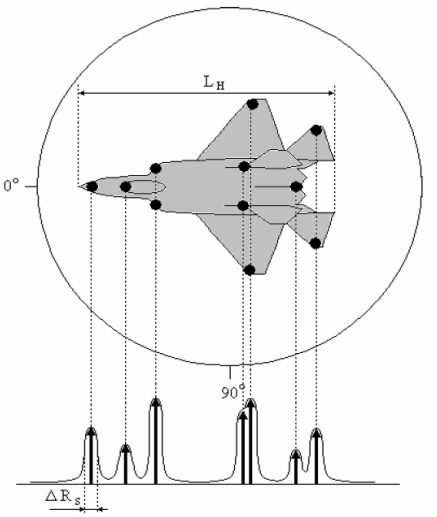

Fig.1: Example of a radar target range profile (HRRP)

In the literature assigned to ATR system theory based on HRRP use, a lot of methods for radar pattern recognition are mentioned. The most part of these approaches has as starting point the basic target 1D HRRP processing [3], [4], [5] but the use of target HRR *imaginary* can be more efficient as well as classification level [6], [7], [8]. However, the classification results offered by all these methods depend on the specific procedure used for target HRRP reconstruction, on the radar information accuracy and perturbation factor influence [2].

According to [8], the more (multispectral) information is available the more effective the ATR process is. As a result a very good option would be to use information coming from several (spectral independent) sensors for *high level fusion* (or *decision fusion*). Having as starting point the current quality of the provided information and classification process that is specific to video imaginary, a *fusion set* of imaginary type {HRR, video} can be very interesting for a further ATR system implementation.

Fusion makes the ATR system not only more powerful but also more robust because different spectral sensors have specific capabilities and robustness at perturbation factors [7].

To implement the decision fusion, several standard models are presented in the literature. However, the major problem of these methods is to develop efficient algorithms to combine the answers given by various classifiers in order to obtain the best results. According to this idea, other approaches, much more systematic, are based on possibility theory, Dempster-Shafer theory, fuzzy logic or Sugeno's fuzzy integral [7], [8].

The aim of this paper is to present a suitable design solution for a more efficient multispectral ATR system based on improved version of Sugeno's fuzzy integral and respectively, target HRR and video imaginary fusion use. All these proposed objectives will be checked against a real database. Therefore, in the first part of the paper a theoretical presentation of the standard and improved fuzzy integral algorithms is made. Then the design procedure for the real database used in unrolled applications is presented. In the last part of the paper, the experimental results that confirm the broached theoretical aspects from beginning are shown. Finally, some conclusions and future research directions in this action field are included.

2 Sugeno's fuzzy integral

Sugeno's fuzzy integral is a non-linear functional, similar to a Lebesgue's integral, defined with respect to a fuzzy measure [7], [8].

Let us consider a set Q and $h:Q\to[0,1]$ a fuzzy subset of this one. Then, the standard fuzzy integral of the function *h* on Q, with respect to the fuzzy measure *g*, is expressed by the equation

$$\int_Q h(q)\circ g(\cdot)=\max_{A\subseteq Q}\left[\min\left[\min_{q\in A}\left(h(q),g(A)\right)\right]\right]=\max_{\alpha\in[0,1]}\left[\min\left(\alpha,g(h_\alpha)\right)\right], \quad (1)$$

where $h_\alpha=\left\{q\,\middle|\,h(q)>\alpha\right\}$.

Function $h(q)$ quantifies the decision taken by the classifier *q* concerning the membership of the unknown target to some class. In other words, this value measures the degree with which the concept *h* is satisfied by *q*.

The term $\min_{q\in A}h(q)$ measures then the degree with which the concept *h* is satisfied by all the elements of the subset *A*. Function $g(A)$ represents the importance of the classifier group constituting the set *A* for the final decision or, in an equivalent way, the degree with which they satisfy the concept *g*.

Consequently, the value obtained by the comparison of the two quantities through the operator *min* will indicate the degree with which the classifier set *A* satisfies the two criteria. One can then conclude that the fuzzy integral looks for the maximum degree of agreement between the real possibilities and expectations, measured by the functions *h* and *g* respectively.

In order to calculate the fuzzy integral, the values $h(q_i)$ are supposed sorted in descending order, by the form: $h(q_1)\ge h(q_2)\ge\ldots\ge h(q_N)$, where *N* is the number of used classifiers. If they are not naturally, one can always change the order of q_i, so that this condition is met. Hence, the fuzzy integral can be calculated with the following equation:

$$\lambda=\int_Q h(q)\circ g(\cdot)=\max_{i=\overline{1,N}}\left[\min\left(h(q_i),g(A_i)\right)\right], \quad (2)$$

where $A_i=\{q_1,q_2,\ldots,q_i\}$.

The value for $g(A_i)$ can be calculated in a recursive way using the following property of any fuzzy measure g_λ:

$$\begin{cases}g(A_1)=g(\{q_1\})=g^1\\ g(A_i)=g^i+g(A_{i-1})+\lambda g^i\cdot g(A_{i-1}),i=\overline{2,N}\end{cases}. \quad (3)$$

Accordingly, the data fusion of the *N* outputs of the *N* classifiers is carried out by the algorithm given below.

S1. *Training stage*

1) Measure the performances of the used classifiers and obtain their fuzzy density function for each class.

The value of $g_j^i=g_j(\{q_i\})$ is considered to be the recognition (or classification) rate of the classifier q_i for the class C_j.

2) For each class C_j, calculate the corresponding value λ_j using the following equation:

$$g(Q)=1\Rightarrow\lambda+1=\prod_{i=1}^{N}\left(1+\lambda g_j^i\right). \quad (4)$$

S2. *Classification stage*

1) Calculate the outputs $o_j^i=h_j(q_i)_{j=\overline{1,m},i=\overline{1,N}}$ of the *N* classifiers corresponding to the *m* classes.

2) Calculate the fuzzy integral for each class with $g_j(A_i)$ determined with the equation (1):

$$\lambda_j=\max_{i=\overline{1,N}}\left[\min\left(o_j^i,g_j(A_i)\right)\right]. \quad (5)$$

3) Decide on the membership of the target according to the rule:

$$\begin{cases} \text{if } \max\limits_{j=1,m} \lambda_j \geq \lambda_0 \text{ and } k = \arg\left[\max\limits_{j=1,m} \lambda_j \right] \\ \qquad \text{then } x \in C_k \\ \text{if } \max\limits_{j=1,m} \lambda_j < \lambda_0 \text{ then } x \text{ is unknown target} \end{cases}, \quad (6)$$

where λ_0 indicates a *confidence* threshold below which the target is declared unknown. It can be considered as the lowest value of the fuzzy integral $\{\lambda_k\}_k$ obtained during the training process.

The block diagram describing the fusion procedure is presented in Fig.2.

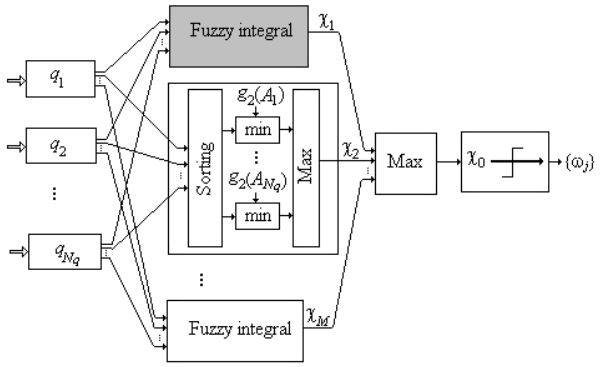

Fig.2: Decision fusion based on standard Sugeno's fuzzy integral use

More details regarding standard fuzzy integral theory and used notations can be found in [7].

3 Fuzzy-evolutive integral

The *fuzzy-evolutive* integral is a hybrid method employed to optimize the mixing mode of the outputs assigned to more (neural) classifiers. This procedure uses the standard fuzzy integral to realize the suitable output combination of some distinctive neural networks based on the importance assigned to them by a proper genetic algorithm.

According to this idea, the chromosomes will *real* encode the fuzzy densities g_i^j as a $C_j = \left(g_1^j, g_2^j, ...; \lambda_j \right)$ vector, and the *fitness* function for C_j will be given by equation:

$$E\left(C_j\right) = \sum_{A \in B(X)} \left| \hat{g}_{\lambda_e}(A) - \right.$$
$$\left. - \frac{1}{\lambda_j} \left[\prod_{x_i \in A} \left(1 + \lambda_j g_i^j \right) - 1 \right] \right|, \quad (7)$$

where $\left\{ \hat{g}_{\lambda_e}(A) \right\}$ are the initial assigned values for fuzzy measures, and $\left\{ g_{\lambda_e}(A) \right\}$ are the calculated values using g_i^j and λ_j.

The basic diagram describing the proposed evolutive fusion method is presented in Fig.3.

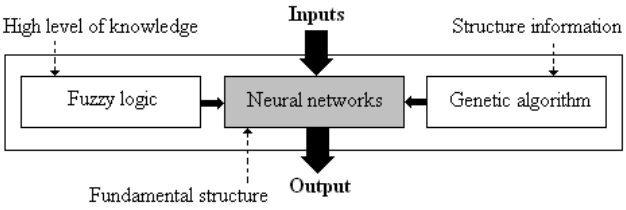

Fig.3: Decision fusion based on fuzzy-evolutive integral use

The *stopping criterion* for the proposed genetic algorithm was represented by the exceeding of the maxim generation number (this number has a constant value) or when the goal error was reached.

The *parents selection* for the next generation was realized using an *elitist* method. In order to eliminate untimely convergence phenomenon, the *fitness* function was scaled acording to the following equation:

$$E_{\max}^{new} = k \cdot E_{\max}^{old}, \; k \in [1.2, 2]. \quad (8)$$

The *crossover* supossed the use of *two* splitting points (randomly chosen), and each chromosome had attached a certain crossover probability with values into $[0.6, 0.95]$ range. In order to introduce new chromosomes inside of the current population, and to protect genetic algorithm against irreversible and accidental information failures generated by improper crossover operations, the *mutation* was used. The probability of mutation was chosen into $[0.001, 0.01]$ range.

Generally speaking, it is known that the solution given by genetic algorithm is coded under the form of the most performant chromosome that belongs to the last generation, but in fact, nothing not garantees us that a more performant chromosome has not been obtained, for example, in the previous chromosomial generation. Consequently, using the analogy with the *Gallant* algorithm from neural network theory, at each chromosomial generation, the best chromosom from this population will be kept into *pocket* and thus, after a suitable decreased order technique, it will result indeed the best final solution.

More details regarding fuzzy-evolutive integral, and assigned genetic algorithm can be found in [8].

4 Database design

To add more consistency to applications developed in the experimental part of this paper, the database was made using the real information given by *two* spectral independent sensors namely, a sensor in *visible* spectrum (a CCD camera), and a HRR sensor (by ISAR type).

Accordingly, the used database will contain the following two target image datasets:

A. the video dataset was obtained using a (digital) photographical survey of *five* military aircraft models (i.e., F 117, Mirage 2000, Mig 29, F16, and Tornado) scaled at 1:48 (see Fig.4). As one can see on Fig.5, the survey was taken using a 5^0 increment in the azimuthal plane, using an angular range of $\left[0^0, 180^0\right]$, justified by the geometric aircraft shape symmetry.

F 117 model

Mirage 2000 model

Mig 29 model

F16 model

Fig.4: Examples of aircraft models used in video database design

Each image from the input video database has a resolution of 520×160 pixels in an uncompressed BMP format.

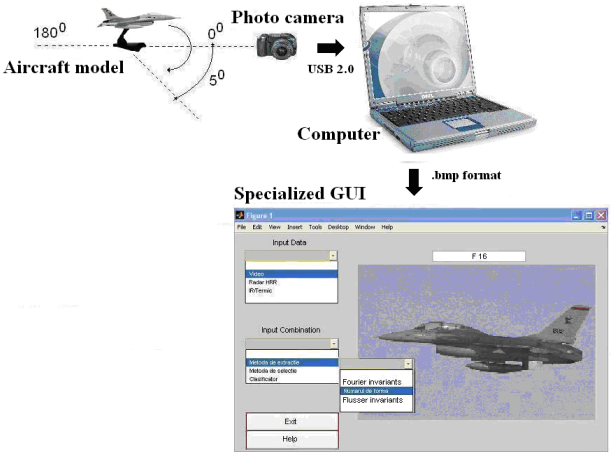

a. Experimental setup

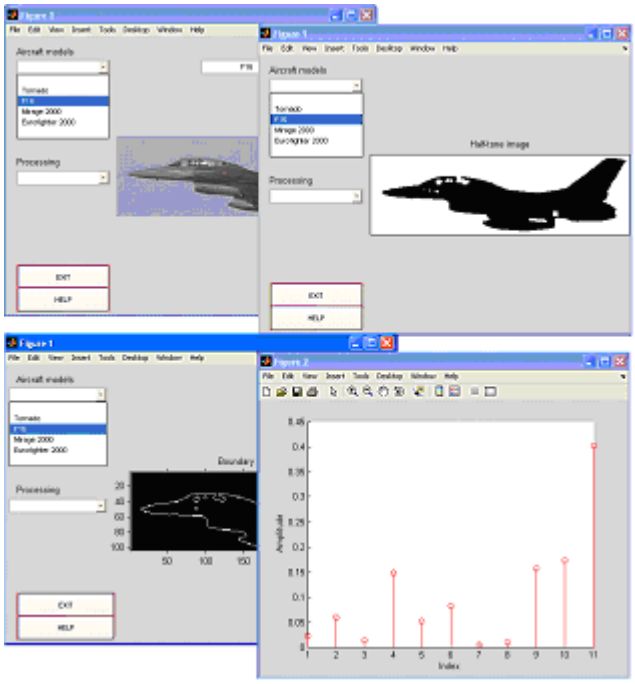

b. GUI designed for preprocessing stage

Fig.5: Basic diagram used in case of video database design

After the acquisition and preprocessing step (see Fig.5), a number of 37 video images/class is obtained. As feature extraction method, the Fourier invariants (most important 11 were retained) were used. Accordingly, the feature vector matrix has the dimension of (11×37) for each interested target.

B. the HRR image *reconstruction algorithm* (for the same military aircrafts) contains the following basic *steps*:

S1) *Primary radar data acquisition and HRRP generation*

The real data were obtained in an anechoic chamber (of MTA/MID laboratory) using the experimental setup shown in Fig.6.

Each target is illuminated in the acquisition phase with a stepped frequency signal. The data snapshot contains 128 frequency steps, uniformly distributed over the band $[11.65,8]$GHz, which results in a frequency increment of $\Delta f = 50$ MHz. Accordingly, the slant range resolution and ambiguity window are given by equation:

$$\Delta R_S = \frac{c}{2B} \cong 3\,\text{m},\ W_S = \frac{c}{2\Delta f} \cong 2.35\,\text{cm} \qquad (9)$$

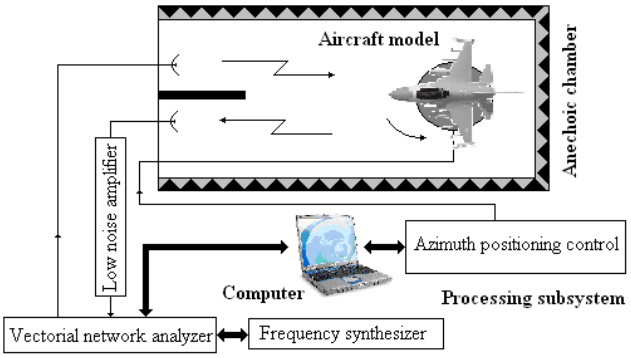

Fig.6: Experimental setup

The *frequency* (*complex*) *signature* obtained from a backscattered snapshot is coherently integrated using IFFT transformation in order to obtain the slant HRRP (HH and VV) corresponding to a given aspect of an interested target. For each of the 5 targets, 201 range profiles are thus generated for 201 angular positions, from -5^0 to 95^0, with an angular increment of 0.5^0. Therefore, for each interested target, the HRRP matrix has the dimension of (128×201).

S2) *Target HRR image reconstruction*

Using spectral analysis in polar coordinates, for measured complex samples, the reflection point projection on a plane which is perpendicular on the target rotation axis, i.e. target radar image (or HRR image), can be obtained.

If the argument sampling is uniform, then Fourier-2D transformation can be applied to the measured dataset. As one can see on Fig.7a, this is true in Cartesian coordinates but is not true in polar coordinates (θ, f).

Therefore, it is necessary that primary input data to be interpolated in Cartesian grid (k_x, k_y) with uniformly sampled data. The new variables are defined as:

$$\begin{cases} k_x = f\cos\theta \\ k_y = f\sin\theta \end{cases}. \qquad (10)$$

Thus, the target HRR image can be obtained applying e.g., Fourier-2D transformation on interpolated data set (see Fig.7b).

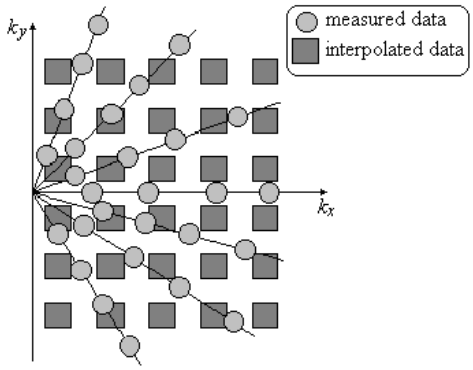

a. Resampling technique for reformatting radar data from polar to Cartesian coordinates

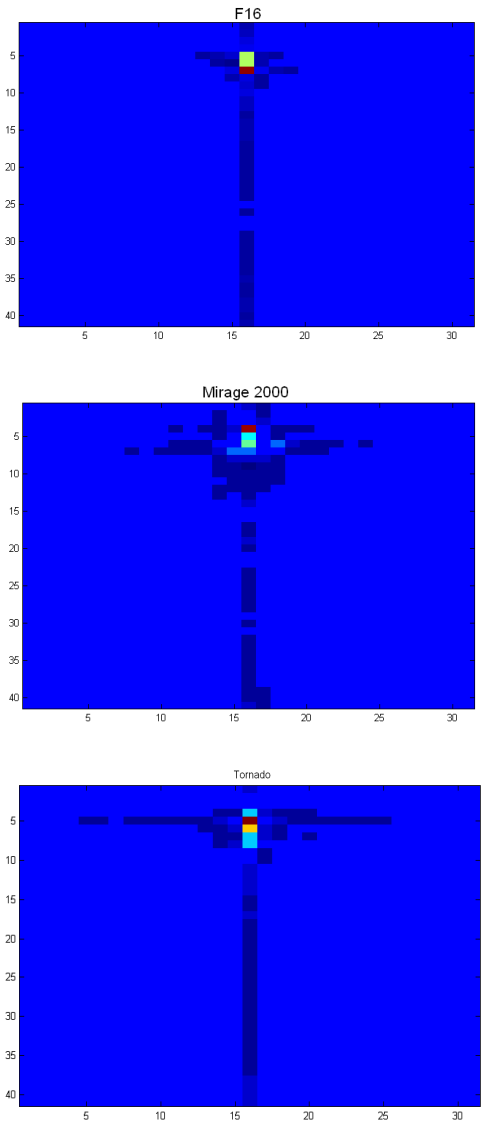

b. Example of target HRR images obtained by Fourier-2D applying

Fig.7: Target HRR image reconstruction using Fourier-2D transformation

S3) *Final form of HRR image dataset*

According to [6], applying Fourier-2D transformation on the HRRP set is not a very good solution to generate target HRR image. It has no good influence on ATR system performance level, as well. However, a more efficient and noise robust solution for classification (recognition) step is represented by ESPRIT-2D *algorithm* applied on the new interpolated dataset [3], [8].

ESPRIT-2D superresolution algorithm provides the *scattering centre locations* of the radar target in the following basic steps [9]:

1) Acquire the data in the frequency-angle domain, resample and interpolate in order to obtain a matrix with uniformly sampled data on a Cartesian grid (see previous step);

2) Estimate the autocorrelation matrix of the data using the spatial smoothing method:

$$R_{ss} = \frac{1}{2L}\sum_{l=1}^{L}\left(\hat{R}_l + J\hat{R}_l^{*}J\right), \tag{11}$$

where $\hat{R}_l = \hat{s}_l \hat{s}_l^H$, s_l is the column vector obtained from the 1^{st} $p_1 \times p_2$ submatrix of the interpolated data matrix and:

$$J = \begin{bmatrix} 0 & \cdots & 0 & 1 \\ 0 & \cdots & 1 & 0 \\ \vdots & \ddots & \vdots & \vdots \\ 1 & 0 & \cdots & 0 \end{bmatrix}. \tag{12}$$

3) Perform the eigenanalysis of the estimated autocorrelation matrix and form the E_{cs} and E_{rs} matrices containing the eigenvectors corresponding to the signal subspace, for the case when the data are processed column by column and row by row respectively;

4) Compute the matrices $F_y = \left(\overline{E}_{cs}\right)^H \underline{E}_{cs}$ and $F_x = \left(\overline{E}_{rs}\right)^H \underline{E}_{rs}$, where $\overline{E}_s$ and $\underline{E}_s$ are obtained from the E_s matrix by eliminating its first and last row respectively;

5) Determine the matrix T which simultaneously diagonalizes the matrices F_x and F_y, i.e.:

$$\alpha F_x + (1-\alpha)F_y = T^{-1}DT, \tag{13}$$

where α is a constant parameter;

6) Apply the transformation T both to F_x and F_y in order to estimate Φ_x and Φ_y:

$$\begin{cases} \Phi_x = T^{-1}F_x^{-1}T \\ \Phi_y = T^{-1}F_y^{-1}T \end{cases}. \tag{14}$$

7) Estimate the scattering centre coordinate pairs (x_k, y_k) using the equations:

$$\begin{cases} \Phi_x = \mathrm{diag}\begin{pmatrix} \exp\left(j\frac{4\pi}{c}\Delta f^x x_{N_1}\right)\ldots \\ \ldots\exp\left(j\frac{4\pi}{c}\Delta f^x x_{N_{sc}}\right) \end{pmatrix} \\ \Phi_y = \mathrm{diag}\begin{pmatrix} \exp\left(j\frac{4\pi}{c}\Delta f^y y_{N_1}\right)\ldots \\ \ldots\exp\left(j\frac{4\pi}{c}\Delta f^y y_{N_{sc}}\right) \end{pmatrix} \end{cases}, \tag{15}$$

where N_{sc} is the number of scattering centers.

More details regarding ESPRIT-2D algorithm theory and used notations can be found in [9].

To generate a single target HRR image (see Fig.8), the HRRP from a 10^0 angular sector was used. After ESPRIT-2D algorithm use, 19 HRR images/class are obtained. It is interesting for the classification step the *polygonal contour* that results using a suitable reunion of the target detected reflection points.

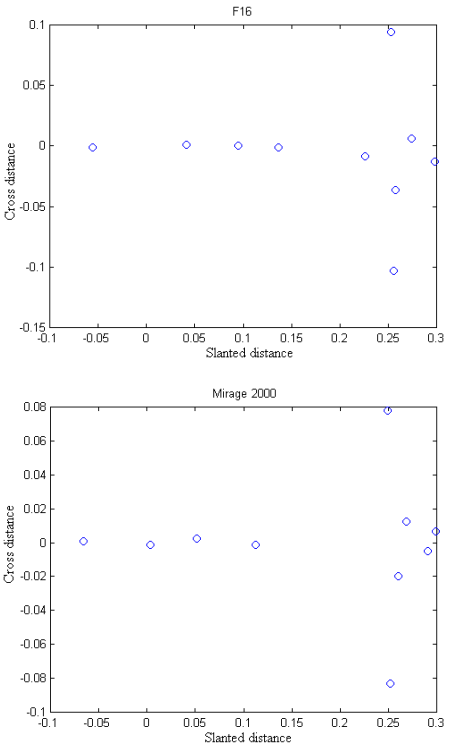

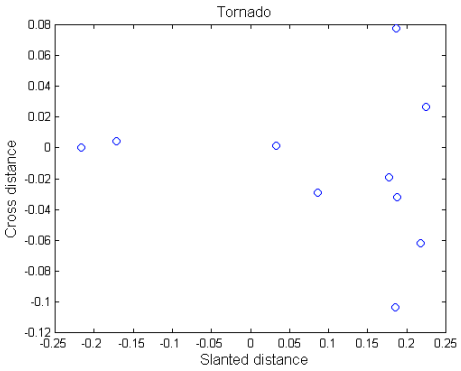

Fig.8: Example of target HRR images obtained by ESPRIT-2D applying

Finally, using a feature extraction algorithm similar with the one from video image case, it results that, for each interesting target, the feature vector matrix has the dimension of (11×19).

More details regarding database design can be found in [10].

5 Experimental results

The main *objectives* of these experiments are:

1) to demonstrate that the modified version of the standard Sugeno's fuzzy integral use leads to improved classification results;

2) to demonstrate that using decision fusion between video image dataset and HRR image datasets results more increased classification scores than the case of 1D HRRP or HRR imaginary singular use;

3) to design specific GUI (in MATLAB) in order to put in evidence the improved performances of the tested multispectral ATR system.

To finalize the (ATR) recognition system form, on feature vector matrix from video case as feature selection method, the Sammon projection algorithm (by $R^{11} \rightarrow R^{n}$ form) was applied [11].

After feature selection step and for each input class, using an interlacing splitting algorithm on resulted matrix with the dimension of (37×5), a number of 19 vectors were used for classifier training while for testing 18 vectors were used.

Finally, a *supervised* ART *artificial neural network* (SART) was used for classification purposes (see Fig.9).

According to [10], SART classifier is developed using q* standard algorithm [11]. It is used a set of prototypes which approximates the probability density modes of the vectors of each input class. The *NN* (*N*earest *N*eighbor) classification rule [12] is then used to classify new vectors compared to these prototypes.

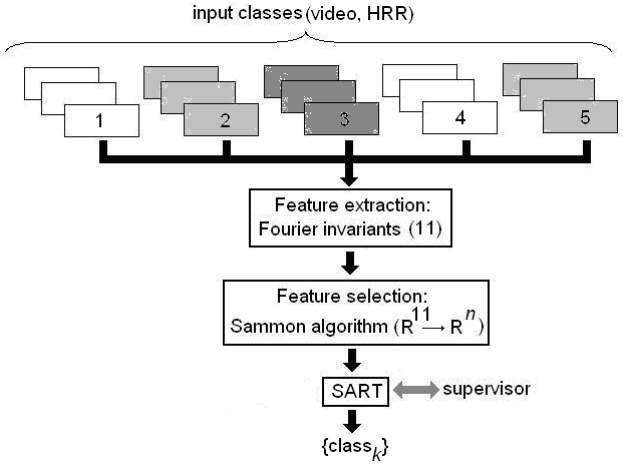

Fig.9: Basic diagram used in the performance testing of ATR system

Generally speaking, this classifier generates in a *supervised* manner a new prototype if the distance between the new vector and the prototype existing yet, exceeds a threshold (according to *Follow the leader* principle from ART artificial neural network theory).

Accordingly, the standard algorithm of SART neural classifier is presented in Fig.10. Finally, the basic steps describing the *working algorithm* of SART classifier are also presented below.

S1) *Initialization stage*

1) Select randomly a vector as prototype for each class from input space.

2) Initialize the vector list associated to each class prototype.

S2) *Training stage*

1) While there are changed prototypes and the error rate is higher than a preset value and for each vector belongs to an input class, compare this vector with the actual prototypes and classified.

2) If the input vector is correct classified, add the vector to the list assigned to the winner prototype.

3) If the vector is not correct classified, declare the vector as new prototype and update the initial vector list.

Update the prototypes assigned to each class. Recalculate the prototypes as average between the vectors that are associated with its own list.

Check if some current prototypes have changed.

Eliminate the prototypes for that associated vector list contains only a vector.

4) Exit if the number of maxim iterations or prototypes is reached.

Calculate the neuronal weights of the output layer using the *pseudo-inverse* method or *Widrow-Hoff* algorithm [12].

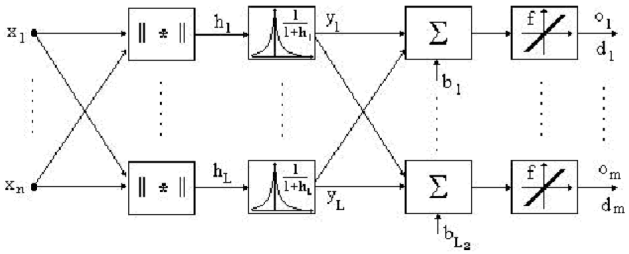

Fig.10: Internal architecture of SART classifier

An important property of the described algorithm is that it needs no initial system parameter specifications and no prespecified number of codebook or center vectors. Indeed, unlike for RBF or LVQ neural networks, the number and the final values of the prototypes are automatically found during the training process for the SART classifier.

More details regarding SART neural network can be found in [10], [11].

In the case of using a HRR dataset, the classification algorithm form is quite similar with the one described above but after applying feature selection, the resulted matrix has the dimension of (19×7). A number of 10 feature vectors were also used for SART classifier training, while for testing 9 feature vectors were used.

To quantify and compare the classification results, the CR (*classification rate*) has been computed (it is the most important performance indicator). The CR represents, in %, the ratio between the number of correct classified input patterns and the total number of used patterns.

Using HH and VV HRR datasets, and after comparative study between two types of decision fusion models, the classification results are synthetically presented in Table 1.

Table 1

Dataset	Classification rate (%)					
	F117	Mirage	Mig 29	F16	Tornado	M
HRR/HH dataset	92	82	85	94	90	**88**
HRR/VV dataset	90	91	83	92	91	**89**
Standard fuzzy integral	94	93	90	97	94	**93**
Fuzzy-evolutive integral	97	96	93	100	96	**96**

Classification results after comparative study

As one can see from Table 1, the proposed modified version of the fuzzy integral has higher values of CR than the standard fuzzy integral.

Also, after applying standard Sugeno's fuzzy integral, its output value variation is synthetically presented in Fig.11.

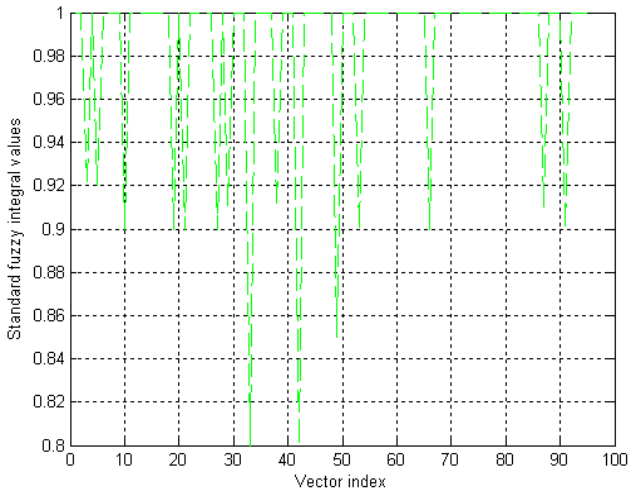

Fig.11: Standard fuzzy integral values during decision fusion process

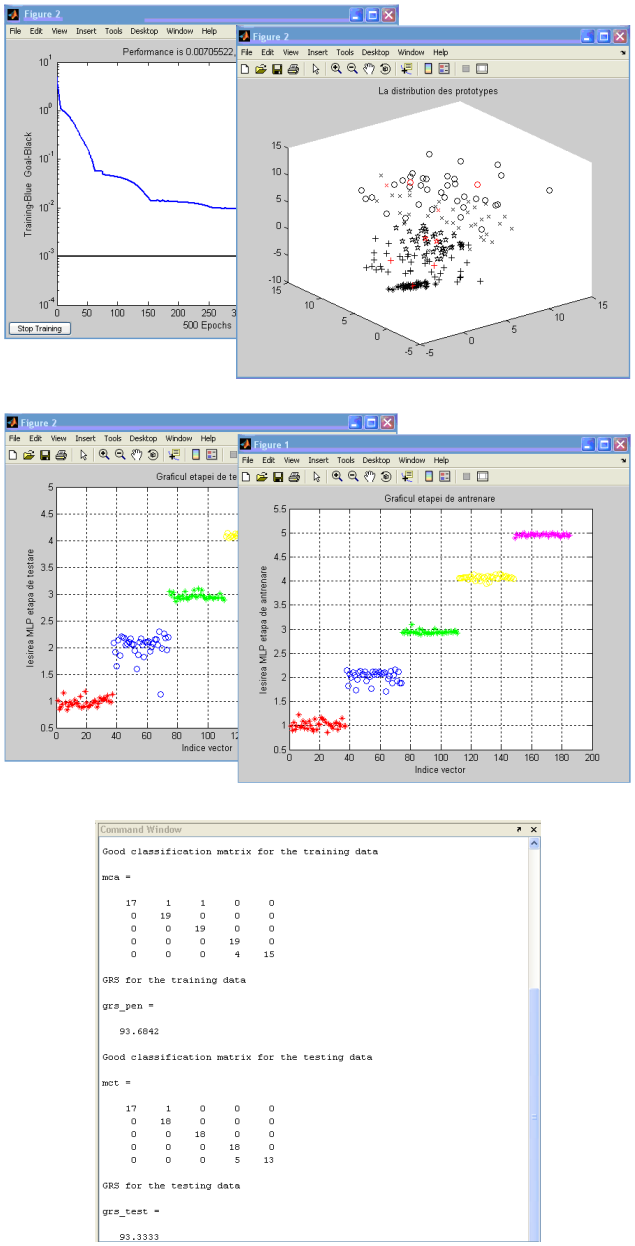

Fig.12: GUI designed for classification stage

Adding to the HRR datasets the video dataset, and using the improved version of Sugeno's fuzzy integral, the obtained experimental results are shown in Table 2.

Table 2

Dataset	Classification rate (%)					
	F117	Mirage	Mig 29	F16	Tornado	M
HRR/HH dataset	92	82	85	94	90	**88**
HRR/VV dataset	90	91	83	92	91	**89**
Video dataset	93	90	91	94	94	**92**
Fuzzy-evolutive integral	100	98	94	100	98	**98**

Classification results after video dataset addition

As one can see from Table 2, the new input dataset use, and fuzzy-evolutive integral applying has as effect higher values of CR than the dataset based only on HRR imaginary use.

All applications presented in this section were developed using MATLAB™ toolboxes *nnet* and *image processing*. Also, in order to implement the proposed genetic algorithm for Sugeno's fuzzy integral optimization, *GAOT* toolbox was used on a Pentium ™ processor at 2.4 GHz.

More explanations regarding experimental aspects treated in this section can be found in [3], [8] and [10].

6 Conclusions and Future Works

The theoretical and experimental results presented in this paper leads to the following *remarks* concerning the efficiency of proposed method for multispectral ATR system performance increase:

1) using the proposed decision fusion method, and HRR imaginary, the CR is improved, generally 3% more than standard fuzzy integral;

2) adding video imaginary to the HRR imaginary, and applying the evolutive version of standard fuzzy integral, the CR is also improved, generally 2% more than radar target image singular use;

3) as a result of the last decision fusion model applying, the obtained classification rates are similar with the ones indicated in the literature [5], [6], [7], namely more than 95%;

4) the computing resources required for fuzzy-evolutive integral calculus are similar with those from the case of standard fuzzy integral use because the genetic optimization of fuzzy densities is not a very expensive time process.

As a final conclusion, a multispectral ATR system that will use the proposed input datasets and the evolutive version of Sugeno's fuzzy integral will be more *efficient* as performance and will have an improved spectral *robustness* at perturbation action.

In a future improvement, the comparative study between presented fusion decision models will be extended to the case of noisy HRRP used in HRR image reconstruction of the target. Also, it is very important to analyze and quantify the influence on ATR system classification performances of SNR or relative error of reflection point positioning.

Another interesting point for a future development refers to the design of an entirely new neural classification algorithms namely, more robust neural networks for feature extraction and selection, and for 2D and 3D classification using different types of imaginaries (e.g., IR/thermic, polarimetric etc.), particularly HRR imaginary.

Finally, in the same scientific research direction is will be interesting to make a serious experimental analysis concerning the design and use of more performing imaginary sensor combinations.

References:

[1] V.G. Nebabin, *Methods and Techniques of Radar Recognition*, Artech House, London, 1994

[2] P. Tait, *Introduction to Radar Target Recognition*, UK: IEE Radar, Sonar and Navigation series, no. 18, 2005

[3] I.C. Vizitiu and L. Anton, "Radar target recognition using range profile", in *Proc. of Int. Conf. on Military Informational Systems. EW and Data Security*, 2005, pp. 263-266

[4] B. Chen, H. Liu, and Z. Bao, "An Efficient Kernel Optimization for Radar High-Resolution Range Profile Recognition", *EURASIP Journal on Advances in Signal Processing*, vol. 2007, article ID 49597, 2007

[5] A.P. Szabo, and P.E. Lawrence, "Target classification using high-resolution range profile", in *Defence Application of Signal Processing*, DSTO Publications, 2005

[6] Quinquis, E. Radoi, and F.Totir, "Some radar imagery results using supperresolution techniques", *IEEE Transactions on Antennas and Propagation*, vol. 52, no. 5, pp. 1230-1244, 2004

[7] Martin and E. Radoi, "Effective ATR Algorithms Using Information Fusion Models", in *Proc. of the 7th Int. Conf. on Information Fusion*, 2004, pp. 161-166

[8] I.C. Vizitiu, "An Application of Fuzzy Integral concerning the Recognition Performance

Increase of Neural Missile Homing System", in *Proc. of 4th Int. Conf. on Radar and ELINT/ESM Systems*, 2007, pp. 231-236

[9] S.Marcos, *Methodes haute resolution*, Hermes Publishing House, Paris, 1998

[10] I.C.Vizitiu, *Neural networks used in video pattern recognition*, Ph.D. Thesis, MTA, Bucharest, 2003

[11] R.O. Duda, P.O. Hart, and D.G. Stork, *Pattern Classification*, New York, USA: John Wiley&Sons, 2001

[12] V.Neagoe, *Pattern recognition and neural networks*, Matrix Rom, Bucharest, 1999